buildings

MDPI

Article

Finite Element Analysis of the Excavation Stability of Deep and Large Ventilation Shafts of Zimuyan Tunnel Using the Raise Boring Machine Method in a Karst Area

Guofeng Wang [1], Fayi Deng [1], Kaifu Ren [1], Yougqiao Fang [1] and Haiyan Xu [2,*]

[1] Guizhou Road and Bridge Group Co., Ltd., Guiyang 550018, China; wangguofeng741321@163.com (G.W.); dengfayi59021@126.com (F.D.); renkaifu398271@163.com (K.R.); fangyongqiao365214@163.com (Y.F.)
[2] School of Civil Engineering, Sichuan Agricultural University, Chengdu 611830, China
* Correspondence: haiyanXU666@163.com

Abstract: The excavation of deep and large vertical shafts in karst areas can easily lead to sudden changes in the stress field of the surrounding rock and even cause disasters such as cave collapses. To investigate the influence of karst areas on the stability of deep and large vertical shaft excavation using the raise boring machine (RBM) method, based on the ventilation vertical shaft project of Zimuyan Tunnel, the influence of karst caves on the displacement and stress fields of the surrounding rock during the construction stage of the vertical shaft was analyzed using the finite element simulation method. Furthermore, the influence of the cave dimensions and the distance between the cave and the shaft on the stability of the surrounding rock was evaluated. The results indicate that the karst cave caused an increase in the radial displacement of the surrounding rock, and the radial displacements and stress in the surrounding rock increased linearly with depth. However, the radial displacement of the surrounding rock in the range of 20*D* to 21*D* (*D* is the well diameter) above the bottom of the well, and the radial stress of the surrounding rock in the range of 7*D* above and below the depth of the cave, are significantly affected by the cave. When the cavern size increased from 0 to 2.0*D*, the maximum radial displacement of the surrounding rock in each construction stage increased by 10.7, 16.6, 2.3, and 2.2 times, respectively. Moreover, when the distance between the cavern and the well was increased from 0.5*D* to 2.0*D*, the maximum radial displacements of the surrounding rock corresponding to each construction stage were reduced by 51.5%, 61.6%, 40.7%, and 18.4%, respectively. These findings can provide valuable references for the design, construction, and monitoring of deep and large vertical shafts in karst areas.

Keywords: finite element analysis; influence law; karst cave; stability; vertical shaft

Academic Editor: Eric M. Lui

Received: 10 December 2024
Revised: 31 December 2024
Accepted: 9 January 2025
Published: 19 January 2025

Citation: Wang, G.; Deng, F.; Ren, K.; Fang, Y.; Xu, H. Finite Element Analysis of the Excavation Stability of Deep and Large Ventilation Shafts of Zimuyan Tunnel Using the Raise Boring Machine Method in a Karst Area. *Buildings* **2025**, *15*, 287. https://doi.org/10.3390/buildings15020287

1. Introduction

The shaft is an important accessory structure for the ventilation function in long and deeply buried traffic tunnels. Under the influence of various unfavorable factors, the stability of the shaft during construction excavation has become one of the challenges in tunnel construction [1,2]. With the development of transportation engineering and the wide distribution of karst, more tunnels need to be built in karst areas [3]. Karst, as an adverse geologic condition affecting the construction safety of underground facilities (e.g., tunnels, shafts), has been of great concern. Therefore, it is necessary to study the excavation stability of deep shafts in karst areas.

A series of studies have been conducted on the stability of shaft excavations. Cheng et al. [4] conducted a series of numerical simulations and proposed a stability control method for the surrounding rock during deep shaft excavation. Hou et al. [5] investigated the effects of high stress, inhomogeneous stratigraphy, and fault structures on the stability of deep shaft excavations and found that the range of the damage zones increased significantly when the wellbore passed through fracture zones or different lithologies. Walton et al. [6] used numerical simulations to understand the factors affecting the relative stability of the two shaft geometries, indicating that variations in shaft geometry are very effective in improving shaft stability. Tangjarusritaratorn et al. [7] performed a three-dimensional finite difference method analysis on the excavation process of deep shafts considering the three-dimensional arch effect and found that previous studies had underestimated the earth pressure acting on the shaft. Wang and Yang [8] carried out on-site monitoring of the construction process of the vertical shaft using the freezing method and analyzed the changing rules of freezing pressure, reinforcement stress, and concrete strain in the well wall. Their results showed that the accumulation of frost heave stresses exacerbated the stresses and deformations in the frozen soil walls, frozen tubes, and shaft walls during shaft excavation. Qiao et al. [9] monitored and analyzed the deformation characteristics of a 56.3 m deep circular shaft and found that excavation was the main factor causing the basement heave, which resulted in vertical movement of the shaft and the surrounding ground surface. Li et al. [2] investigated shaft lining damage incidents in the Huanghuai region of China, and the results showed that the main damage mode of the shaft lining is shear failure. Sun et al. [10] simulated the deformation and stress characteristics of the surrounding rock and shaft lining under the geological conditions of soft–hard rock strata based on the 3DEC program and found that stress concentration and bending moments are easily generated at the interface between soft and hard rock layers. Zhang et al. [11] used numerical simulation to investigate the influence of key rock mechanical parameters on the stability of the surrounding rock in deep shafts and proposed a method for estimating the stability of the surrounding rock. However, most of the current studies have not investigated the stability of excavation of deep shafts in karst areas.

Zimuyan Tunnel is 7.4 km long and has been planned to be constructed with one ventilation shaft, which was opened by the raise boring machine (RBM) method. However, the RBM method excavates in the direction opposite to the direction of gravity of the rock mass, which is significantly different from the excavation method for general shafts and tunnels [12]. In this paper, ABAQUS finite element software (version 6.14) was employed to numerically simulate the excavation stability of the ventilation shaft of Zimuyan Tunnel in the karst area. By considering the existence of karst caves, an analysis was conducted on the displacement and stress fields of the surrounding rock during the construction stage using the RBM method. Furthermore, the deformation patterns were analyzed for different cave sizes and cave–shaft spacing, and the effect of the presence of the cave on the stability of the shaft excavation was evaluated. These findings provide technical references for the design and construction of deep and large vertical shafts in karst areas.

2. Project Overview

Zimuyan Tunnel is located in the junction position of Chongqing City and Guizhou Province, which is a controlling project of the Wulong-Daozhen Expressway. Considering the climate, topography, geological conditions, and traffic conditions of the tunnel siting area, one ventilation shaft is constructed on the right side of the right hole of Zimuyan Tunnel. The shaft is 428.2 m deep and 6.4 m in diameter (D), which is the first deep and large shaft in the Guizhou highway tunnel. Figure 1 illustrates a three-dimensional schematic of the Zimuyan Tunnel shaft. Because the large depth of this shaft leads to low slagging

efficiency via the positive shaft method, and there are certain safety hazards, the shaft is considered to be constructed by the RBM method.

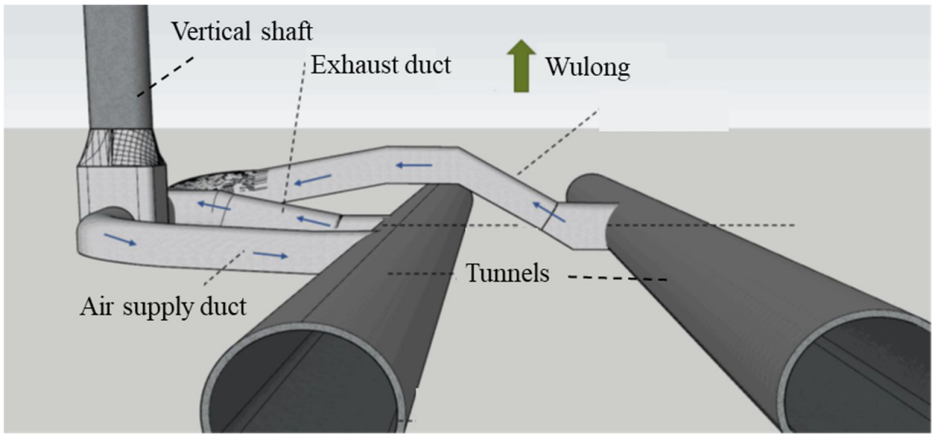

Figure 1. Three-dimensional schematic diagram of the vertical shaft of Zimuyan Tunnel.

The strata of the vertical shaft excavation site are composed of clay (thickness of 0–0.5 m), medium weathered limestone mixed with mudstone (depth of 0.5–165 m), and medium weathered limestone. The topographic and geologic profile of the ventilation shaft of Zimuyan Tunnel is shown in Figure 2. Two karst fissures at depths of 370.4–370.7 m and 374.8–375.0 m were revealed by drill hole data. The possibility of encountering hidden karst during vertical shaft construction is extremely high; thus, the engineering risk is extremely high. In addition, the karst caverns are prone to hazards such as gushing water, sudden mud, and toppling. Therefore, it is necessary to strengthen the monitoring and geological advance prediction and forecasting during construction. The development of karst morphology was found to be very complex during the construction of the shaft, as shown in Figure 3.

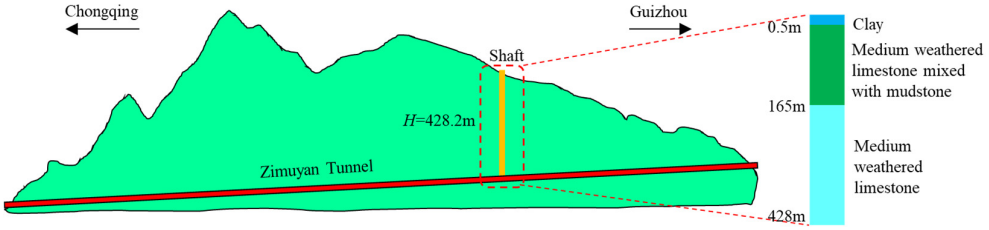

Figure 2. Topographic and geological profile of the ventilation shaft of Zimuyan Tunnel.

Figure 3. Karst development pattern in the vertical shaft.

To investigate the stability of the surrounding rock of the vertical shaft excavated by the RBM method in the karst area, a series of simulations were carried out in this paper using ABAQUS finite element analysis software. The flowchart of this study is shown in Figure 4.

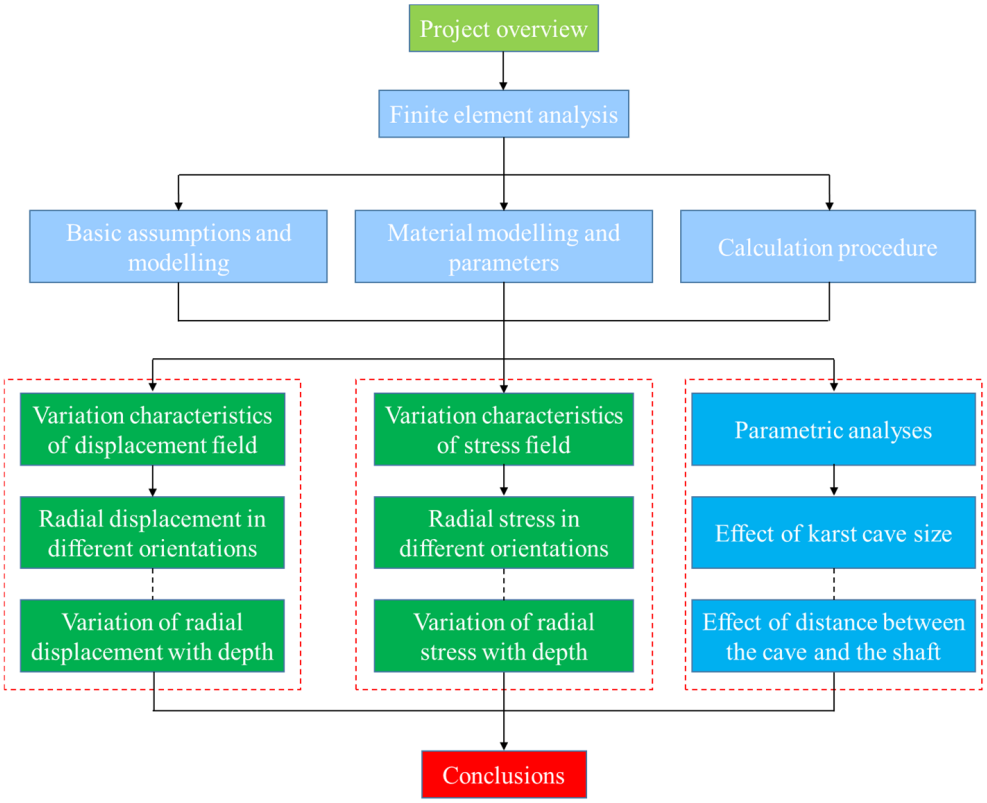

Figure 4. Flowchart of this study.

3. Finite Element Analysis

3.1. Basic Assumptions and Modeling

To analyze the effect of karst on the stability of deep and large vertical shaft excavation, a series of three-dimensional numerical models were established by using the finite element analysis software ABAQUS. Considering the symmetry of the calculation model, half of the shaft excavation model can be established to save the calculation costs [13]. The dimensions of the three-dimensional model are 100 m × 50 m × 428 m (length × width × height). The three-dimensional numerical model is shown in Figure 5. Since the model size is 15.6 times the diameter of the shaft, the influence of boundary effects on the simulation results can be ignored [14]. According to the drilling data, the cavern was set at a depth of 370 m. Karst shapes are usually highly irregular, and the shape of the cavern is simplified to a square [15]. Therefore, it is assumed that the side length of the square cavern is 0.5D (D is the diameter of the shaft) and the minimum distance between the cavern and the shaft is 0.5D, and the effect of groundwater and other fillers is not considered. Horizontal constraints are applied around the entire model, horizontal and vertical constraints are applied at the bottom of the model, and the top of the model is a free boundary. Moreover, the whole model is divided into 41,974 elements and 47,520 nodes.

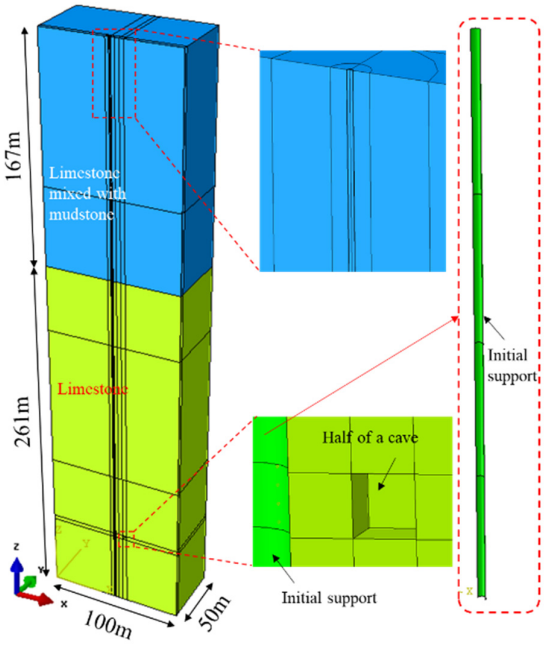

Figure 5. Three-dimensional numerical model.

3.2. Material Modeling and Parameters

Compared to the depth of the shaft, the effect of 0.5 m thick clay on the stability of the shaft excavation is negligible. Therefore, only two layers of surrounding rocks (i.e., medium weathered limestone mixed with mudstone and medium weathered limestone) are considered in this numerical simulation. The Mohr–Coulomb constitutive model was used for the surrounding rock [16]. The initial support was simulated using a shell element, and its material was considered as a linear elastic constitutive model. Borehole coring of the strata was carried out at the site to obtain the distribution of the strata and the basic mechanical parameters of the surrounding rocks. Photographs of the field drill core are shown in Figure 6. Table 1 lists the physical and mechanical properties of the materials. In the finite element analysis, the parameters of the surrounding rock were set to be consistent with the prototype to maximize the accuracy of the predicted results. The anchor reinforcement support effect in vertical shaft excavation can be equivalently achieved by increasing the internal friction angle and cohesion of the surrounding rock-reinforced zone by 20% [17]. Therefore, in this study, the internal friction angle and cohesion of the surrounding rock-reinforced zone were increased by 20% to consider the reinforcing effect of the anchors. In addition, the tie contact relationship between the initial support and the surrounding rock was used to simulate the interaction between the well wall and the surrounding rock. This study mainly considers the stability of the surrounding rock during shaft excavation, and the secondary lining as a safety reserve is not currently considered.

Table 1. Physical and mechanical properties of materials.

Name	Density/(g/cm^3)	Elastic Modulus/GPa	Poisson's Ratio	Internal Friction Angle/(°)	Cohesion/MPa
Limestone mixed with mudstone	26.37	3.2	0.29	38	5.1
Limestone	26.46	3.3	0.28	47	6.0
Initial support	25	35	0.22	—	—

Figure 6. Photographs of drill core (167~173 m as an example).

3.3. Calculation Procedure

Before simulating the excavation, self-weight was applied to the model to generate initial ground stresses. Moreover, the initial ground stress field of the rock considers only the self-gravitational stresses and not the tectonic stresses. As mentioned earlier, the shaft was constructed using the RBM method. Specifically, a pilot hole with a diameter of 0.23 m was excavated, and then the pilot hole was enlarged to a diameter of 0.27 m. Subsequently, a well hole with a diameter of 1.6 m was excavated using the RBM method. Finally, a 6.4 m diameter borehole was excavated in the forward direction, and a 0.5 m thick initial support was applied after each excavation step.

4. Results and Analysis

4.1. Characteristics of Changes in the Displacement Field

4.1.1. Effect of Karst Caves on the Radial Displacement of the Surrounding Rock

For the purpose of analysis and illustration, Figure 7 shows the schematic layout of monitoring points for the radial displacements and stresses of the surrounding rock. Figure 8 illustrates the radial displacement of the surrounding rock at different construction stages.

As can be seen from Figure 8, the radial displacement of the surrounding rock at different construction stages without the influence of the cavern is uniformly distributed and increases with the construction progress. Under the action of the cavern, the radial displacement of the surrounding rock in the pilot hole construction stage decreases gradually with the increase in radial orientation. This phenomenon indicates that the farther away from the location of the cavern, the less the effect on the radial displacement of the surrounding rock. However, compared to the case without karst caves, there was a significant increase in the radial displacement of the surrounding rock during the pilot hole construction stage. The maximum radial displacement during this process increased by 0.63 mm, which occurred at orientation 0, the closest to the cave. During the construction stage when the pilot hole was enlarged, there was a further increase in the radial displacement of the surrounding rock. The maximum radial displacement increased by 1.34 mm compared to the case without karst caves. Moreover, the radial displacement of the surrounding rock varies less with radial orientation in the reaming construction stage compared to the pilot hole construction stage. This can be attributed to the pressure relief effect of the pilot hole, which reduces the surrounding rock pressure around the vertical shaft. It is noteworthy that during the reverse drilling stage, the presence of the caves resulted in highly irregular variations in the radial displacement of the surrounding rock with radial orientation. Deformation concentration occurred in the 45° and 135° orientations,

corresponding to an increase in radial displacement of the surrounding rock by 2.25 mm and 1.02 mm, respectively. The radial displacement of the surrounding rock in the positive construction stage was distributed in a quadrangle star, but the overall distribution was basically close to the circular distribution without caves, which indicated that the initial support played a good reinforcing effect in this study.

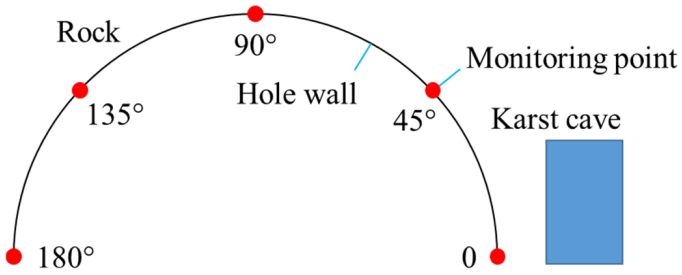

Figure 7. Schematic layout of monitoring points.

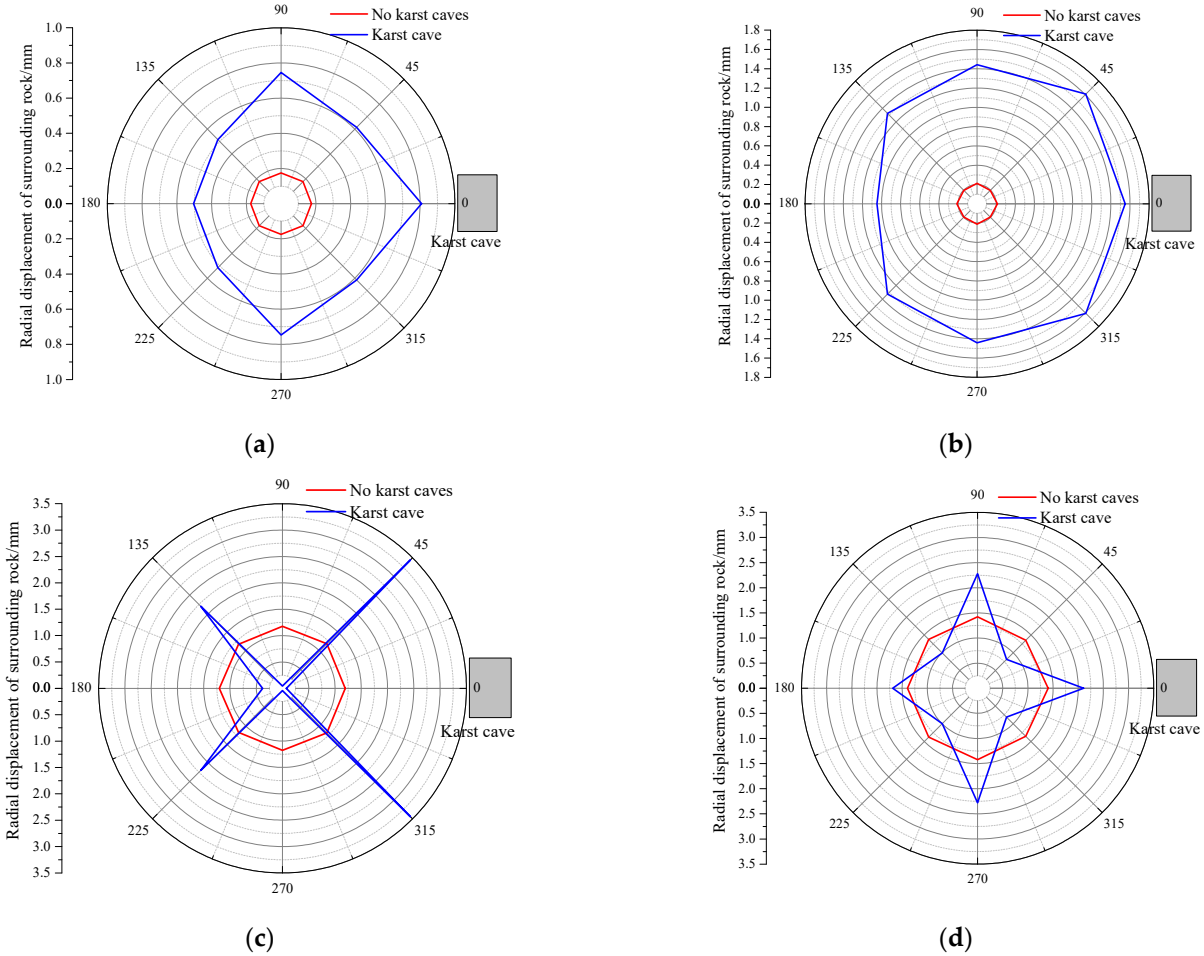

Figure 8. Radial displacement of the surrounding rock at different construction stages: (**a**) pilot hole stage; (**b**) re-expansion stage; (**c**) reverse drilling stage; (**d**) forward drilling stage.

4.1.2. Variation of Radial Displacement of the Surrounding Rock with Depth

To further investigate the variation in the radial displacement of surrounding rock with depth under the action of caves, Figure 9 shows the variation in the radial displacement of surrounding rock with depth at different construction stages and compares it with the case of no cavern. From Figure 9, it can be seen that in the absence of karst caves, the radial displacement of the surrounding rock increases linearly with depth. In the

construction stage of the pilot hole, re-expansion hole, and reverse drilling, the influence of the cavern on the radial displacement of surrounding rock mainly occurs in the range of 20*D*–21*D* above the bottom of the well, and the radial displacement of surrounding rock in other ranges is consistent with the case of no cavern. Compared to the absence of karst caves, the maximum radial displacements increased by 0.178 mm, 0.243 mm, 0.402 mm, and 0.235 mm for the pilot hole, re-expansion hole, reverse drilling, and forward drilling stages, respectively. Within the influence range of the karst cave, the radial displacement of the surrounding rock changed significantly at different radial orientations and depths. Specifically, deformation concentration occurred at the depth of the cave location, which could lead to risks such as wellbore collapse. Therefore, real-time monitoring of radial displacement of surrounding rock should be emphasized in the excavation process of vertical shafts in karst areas using the RBM method, which helps to predict the location of the cavern and reduce the construction risk. The structural integrity of the shaft was ensured by filling the cavern in advance to minimize the effect of the cavern on the radial displacement [5]. Compared to the other construction stages, the radial displacement of the surrounding rock in the forward drilling stage is basically consistent with the radial displacement of the surrounding rock with depth in the case of no cavern. As mentioned earlier, it is attributed to the reinforcing effect of the initial support restraining the deformation of the surrounding rock, thus reducing the influence of the karst cave.

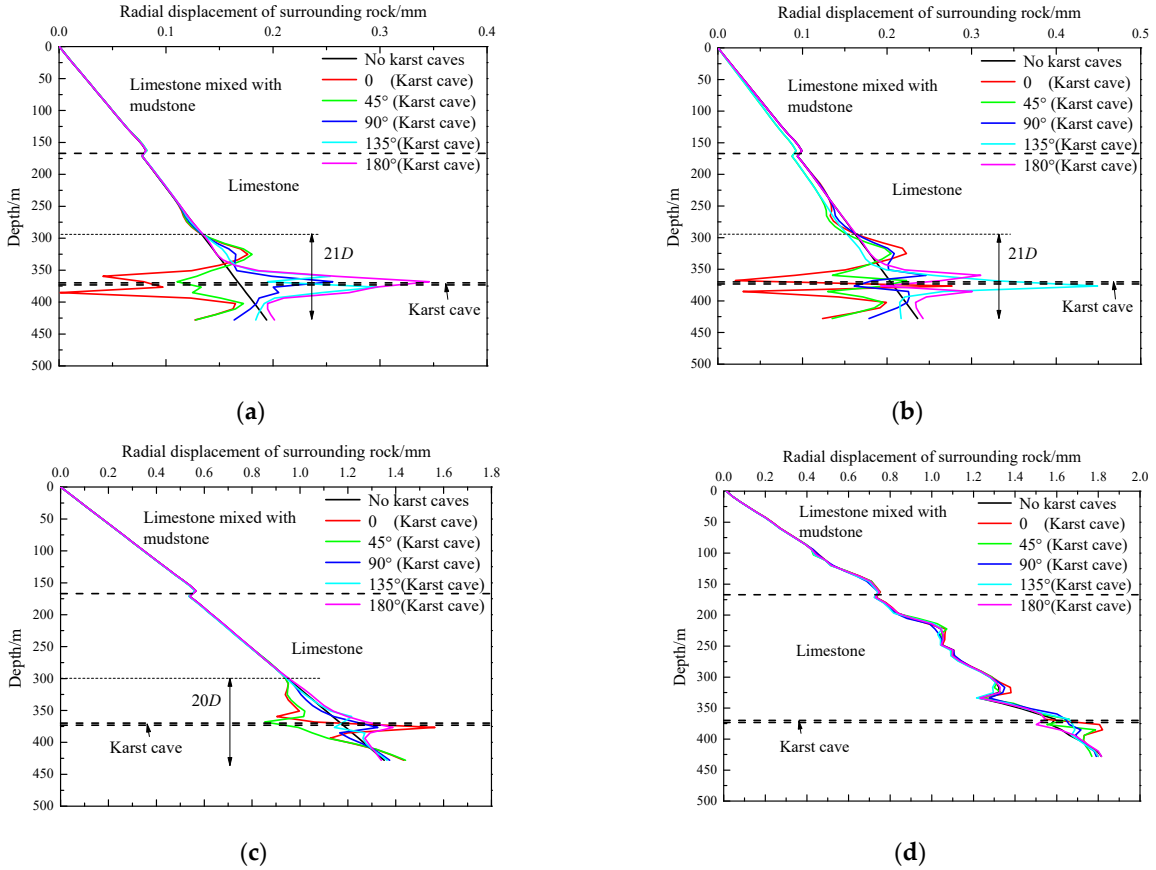

Figure 9. Variation in radial displacement of surrounding rock with depth at different construction stages: (**a**) pilot hole stage; (**b**) re-expansion stage; (**c**) reverse drilling stage; (**d**) forward drilling stage.

4.2. Characteristics of Changes in the Stress Field

4.2.1. Effect of Karst Caves on Radial Stresses in the Surrounding Rock

The cross-section of the shaft excavation at the same depth as the cavern was selected to analyze the radial stress pattern of the surrounding rock with or without the action of

the cavern, as shown in Figure 10. The cavities lead to an asymmetric distribution of radial stresses in the surrounding rock at the equal depth. This asymmetric stress distribution easily leads to stress concentration, which causes large deformation of the well wall and even collapse damage. Throughout the construction stage of the shaft using the RBM method, the influence of the cavern on the radial stresses in the surrounding rock mainly occurs during the construction stage of the pilot hole. The cavern reduced the radial stress in the surrounding rock during the construction stage of the pilot hole, with a maximum reduction of 1.2 MPa, located in the orientation 0 closest to the karst cave. Subsequently, the effect of the cavern on the radial stresses in the surrounding rock is less and decreases the further away from the cavern. This can be attributed to the fact that the pressure relief in the pilot hole stage reduces the influence of the surrounding rock pressure and karst caves.

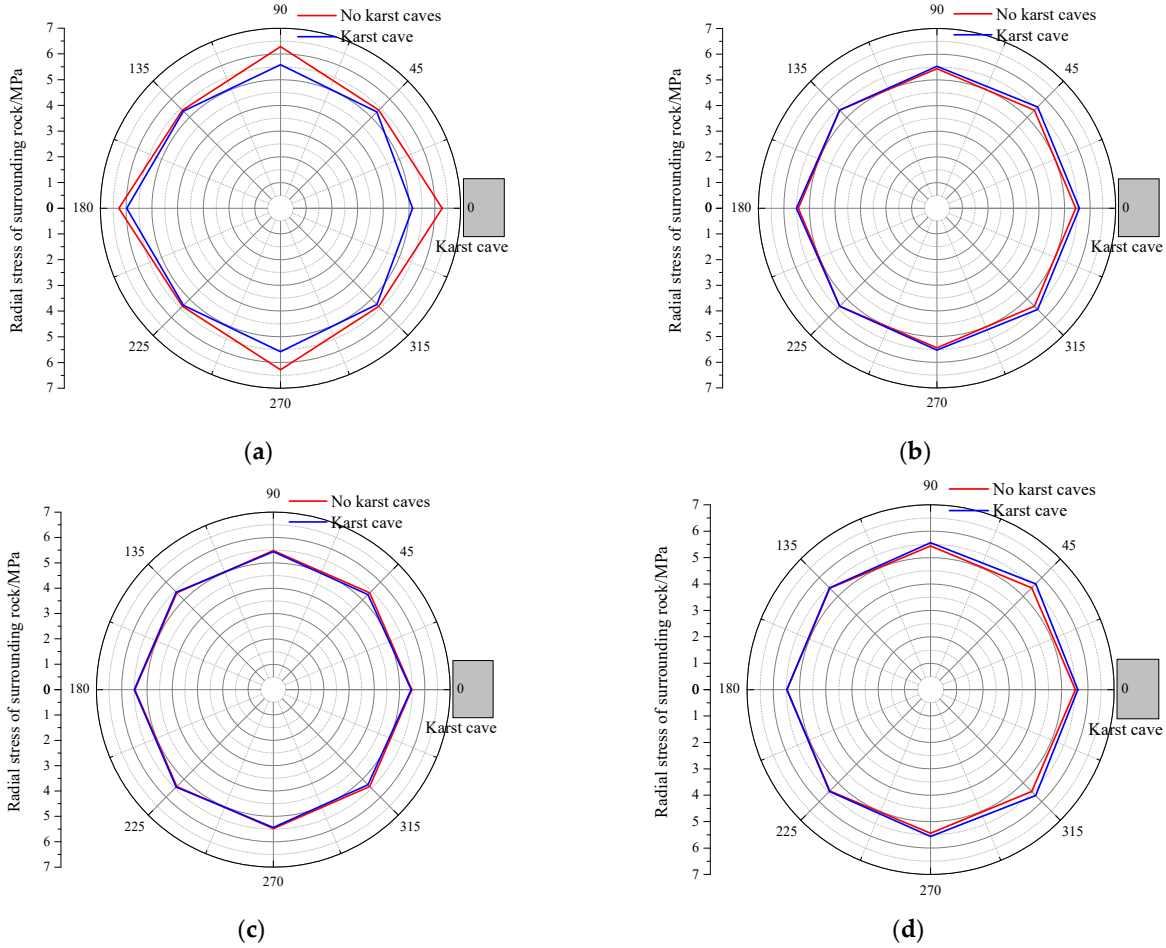

Figure 10. Radial stress of the surrounding rock at different construction stages: (**a**) pilot hole stage; (**b**) re-expansion stage; (**c**) reverse drilling stage; (**d**) forward drilling stage.

4.2.2. Variation in Radial Stress of the Surrounding Rock with Depth

To further analyze the variation of radial stress of surrounding rock with depth under the action of karst caves, Figure 11 depicts the variation law of radial stress of surrounding rock with depth at different construction stages. During the excavation stage of the vertical shaft, the radial stress of the surrounding rock without karst caves increases linearly with depth [7]. It is noteworthy that a sudden change in stress occurs at the interface between soft and hard rock layers. This similar observation is consistent with a previous study carried out by Sun et al. [10]. The radial stresses of the surrounding rock in the range of 7*D* above and below the depth of the cavern location were significantly affected by the cavern,

and the radial stresses of the surrounding rock at other depths were in good agreement with the variation pattern in the absence of the cavern. The effect of the cavern on the radial stresses in the surrounding rock is most significant during the construction stage of the pilot hole. Compared to cases without karst caves, the radial stress of the surrounding rock decreases sharply. Therefore, in order to avoid drill bit jamming and deflection during the pilot hole construction stage, the drill hole inclination test should be carried out in real-time.

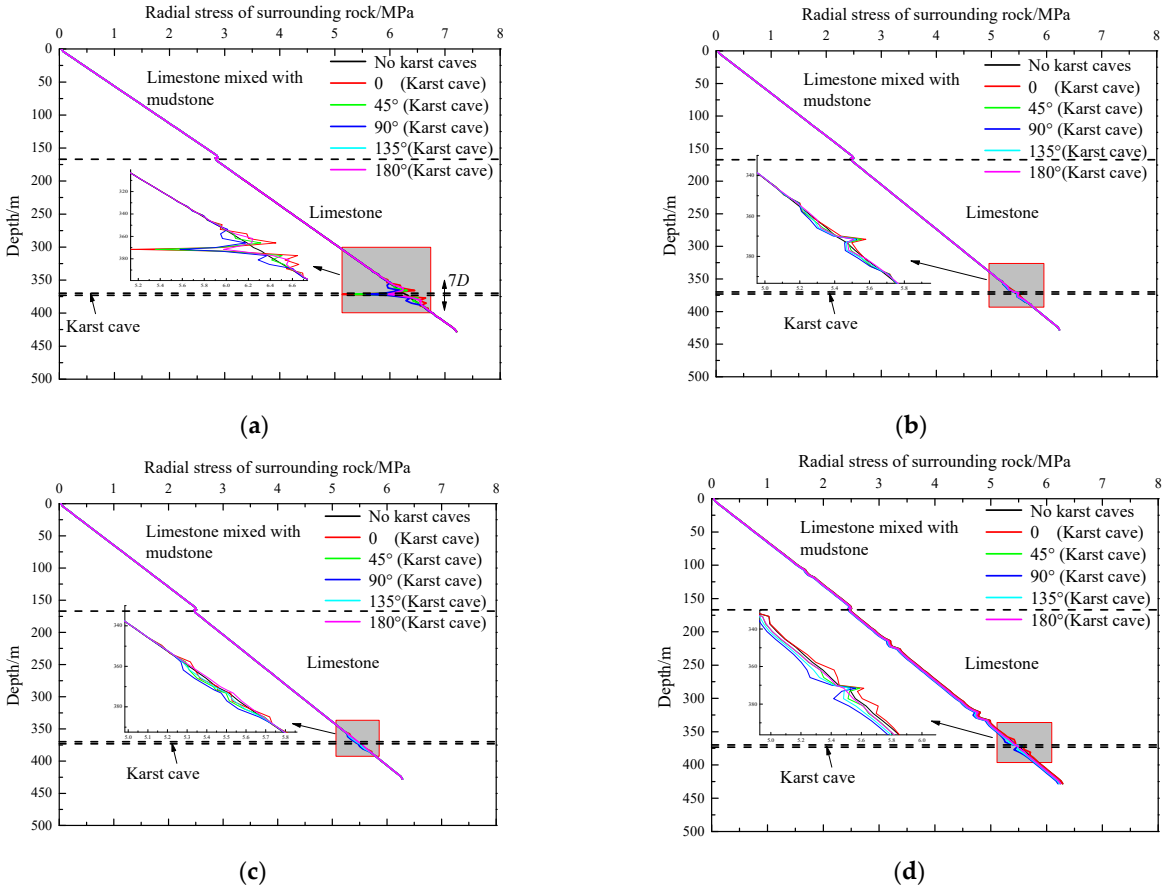

Figure 11. Variation in radial stress of surrounding rock with depth at different construction stages: (**a**) pilot hole stage; (**b**) re-expansion stage; (**c**) reverse drilling stage; (**d**) forward drilling stage.

5. Parametric Analyses

In order to investigate the effect of cavern size and cavern–shaft spacing on the stability of the surrounding rock, six sets of numerical analyses were performed in this study. The calculated cases are shown in Table 2.

Table 2. Calculated cases.

No.	Cave Size	The Distance Between Karst Cave and Vertical Shaft
1	0	0.5*D*
2	1.0*D*	0.5*D*
3	1.5*D*	0.5*D*
4	2.0*D*	0.5*D*
5	1.0*D*	1.0*D*
6	1.0*D*	2.0*D*

5.1. Effect of Karst Cave Size

Figure 12 demonstrates the effect of increasing the size of the cavern from 0 to 2.0*D* on the radial displacement of the surrounding rock at different construction stages. As the size of the cavern increases, the effect of the cavern on the radial displacement of the surrounding rock becomes more pronounced. The radial displacements of the surrounding rock in different radial orientations have a consistent distribution pattern at the same construction stage and the radial displacements of the surrounding rock increase with the increase in the cavern size. Under the influence of the cavern, the closer to the cavern, the greater the change in radial displacement of the surrounding rock. When the size of the cavern increased from 0 to 2.0*D*, the radial displacement of the surrounding rock in orientation 0 increased by 10.7, 16.6, 2.3, and 2.2 times in the pilot hole, re-expansion hole, reverse drilling, and forward drilling stages, respectively. Therefore, the drilling inclination test should be conducted in the pilot hole and re-expansion stages to prevent the influence of the cavern from causing the drilling deflection. Moreover, the radial displacement of the surrounding rock varies greatly at different orientations during the reverse drilling stage, and attention should be paid to the deformation concentration that may cause collapse.

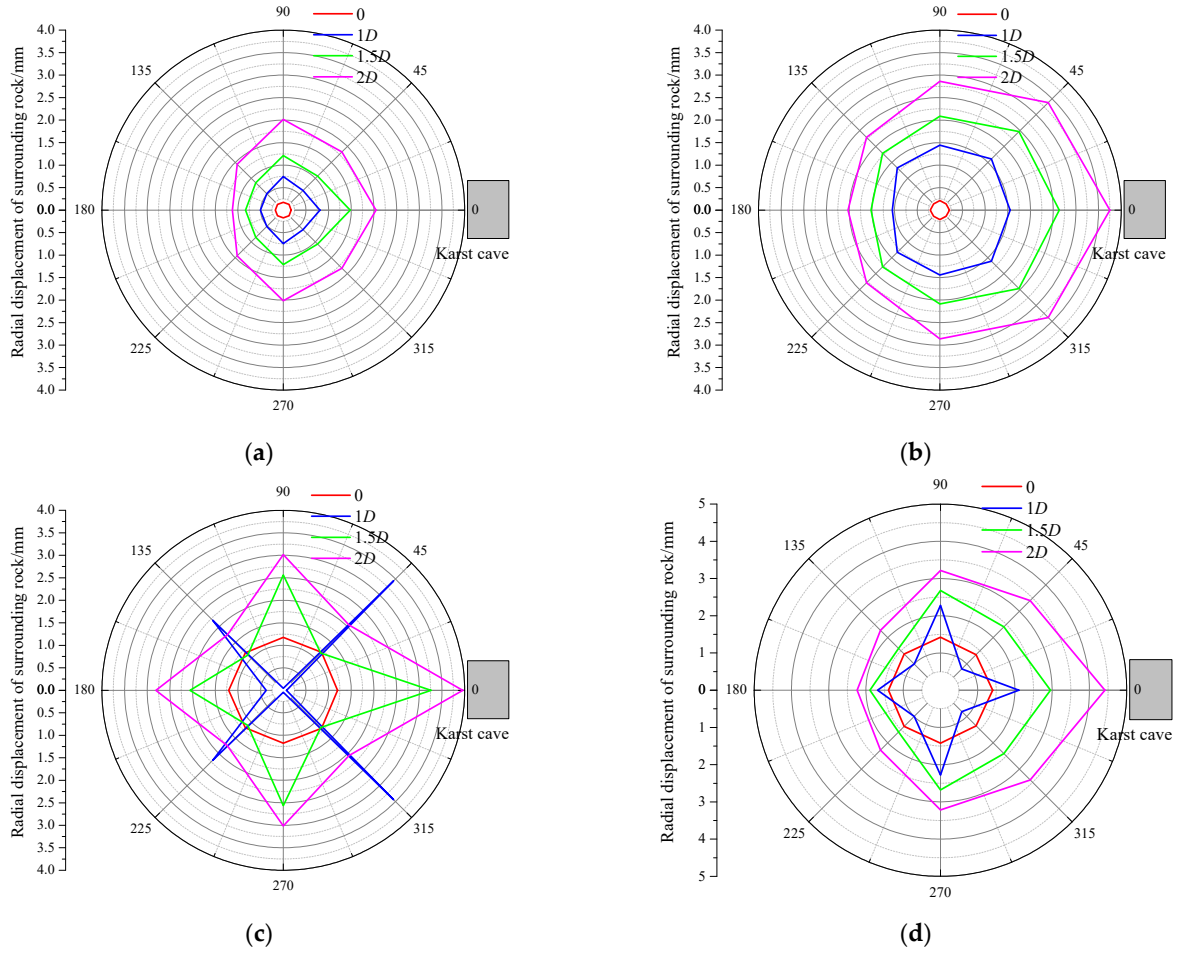

Figure 12. Influence of cave size on radial displacement of surrounding rock under different construction stages: (**a**) pilot hole stage; (**b**) re-expansion stage; (**c**) reverse drilling stage; (**d**) forward drilling stage.

5.2. Effect of Distance Between the Cave and the Shaft

In addition to the size of the cave, the distance between the cave and the well has a significant effect on the stability of vertical shaft excavation. Figure 13 shows the effect of the distance between the cavern and the shaft on the radial displacement of the surrounding

rock under different construction stages. The larger the distance between the cavern and the well, the smaller the radial displacement of the surrounding rock at different construction stages. The effect of the distance between the cavern and the well on the radial displacement of the surrounding rock is more significant in the pilot hole and re-expansion stages. As mentioned earlier, the radial displacement of the surrounding rock varies greatly at different orientations during the reverse drilling stage. During the forward drilling stage, the effect of the cavern on the radial displacement of the surrounding rock is less due to the initial reinforcement. When the distance between the cavern and the well was increased from 0.5*D* to 2.0*D*, the maximum radial displacements of the surrounding rock corresponding to each construction stage were reduced by 51.5%, 61.6%, 40.7%, and 18.4%, respectively. Therefore, the construction of deep and large vertical shafts should be avoided as much as possible within 2.0*D* from the karst area, and construction monitoring and early warning should be carried out.

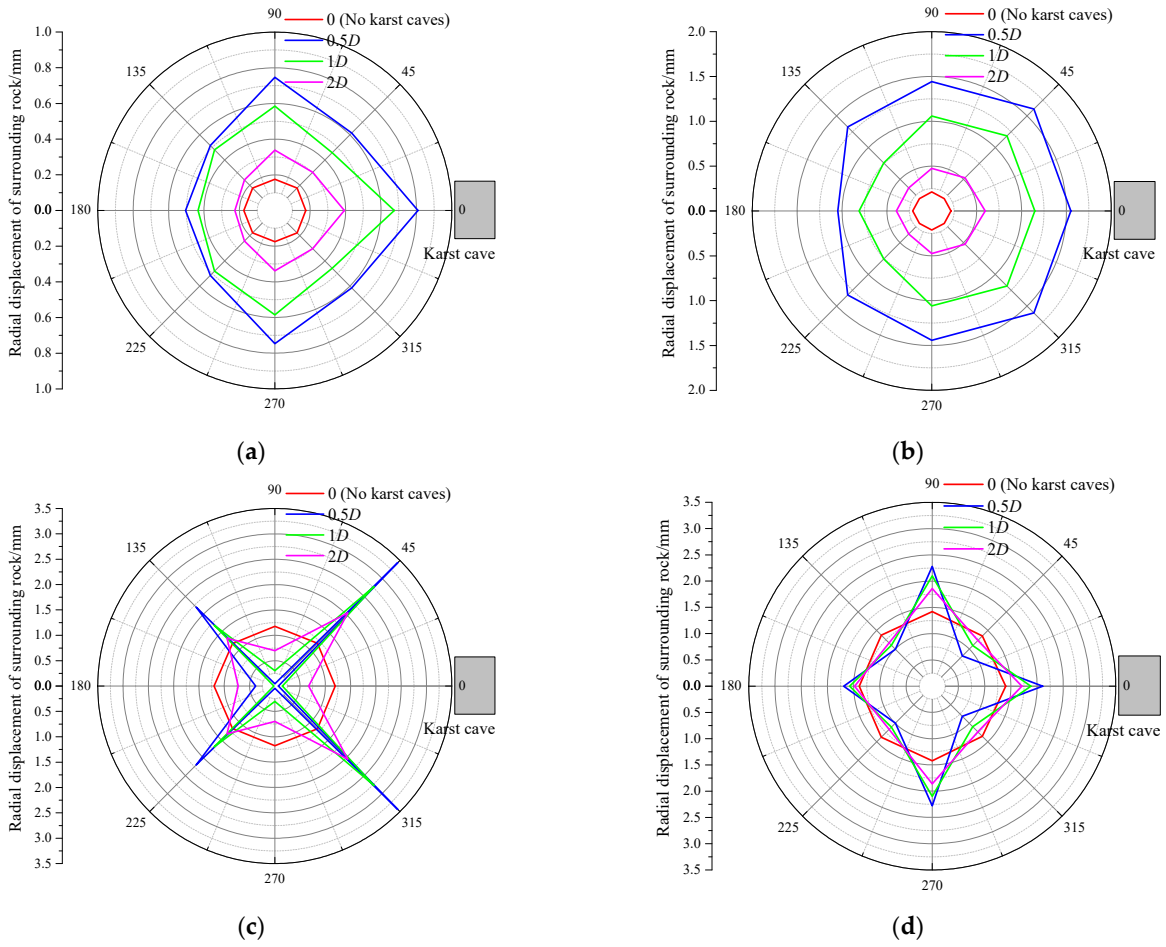

Figure 13. Influence of the distance between the cavern and the shaft on the radial displacement of the surrounding rock under different construction stages: (**a**) pilot hole stage; (**b**) re-expansion stage; (**c**) reverse drilling stage; (**d**) forward drilling stage.

6. Discussion

This study reveals the influence of karst caves on the displacement and stress fields of the surrounding rock during vertical shaft construction using the RBM method and evaluates the influence pattern of the cave size and the distance from the cave on the stability of the surrounding rock. Compared to the case without karst caves, karst caves have a significant effect on the radial displacement and stress of the surrounding rock.

These findings were useful in predicting the location of the cavern and ensuring the stability of the surrounding rock for the shaft excavation.

This study also has some limitations due to space constraints. For example, this study did not consider the effect of water-filled caverns on the stability of the surrounding rock during shaft excavation. During construction, no water-filled cavities were found (Figure 3). It is noteworthy that fewer studies have examined the stability of caverns on the surrounding rock during shaft excavation. A series of studies have been conducted on the stability of the surrounding rock during the excavation of karst tunnels by hidden caves [15,18,19]. However, these studies also did not consider the cases of water-filled caves. Previous studies have investigated the effects of cave shape, cave size, and the distance between the tunnel and the cave on the stability of the surrounding rock [15,20,21]. Generally speaking, karst areas have abundant groundwater, which is the main factor affecting the stability of geotechnical engineering [22]. Therefore, the effect of groundwater on the stability of the surrounding rock during shaft excavation deserves to be focused on in subsequent studies. Moreover, field deformation monitoring was also an effective means to investigate the deformation failure mechanism of vertical shafts [15,23]. Therefore, during the forward excavation stage of the shaft, the surrounding rock deformation and lining stresses should be monitored to prevent wall collapse caused by cavities.

7. Conclusions

In this paper, ABAQUS finite element analysis software was used to analyze the variation characteristics of radial displacement and stress of surrounding rock during the excavation process of vertical shafts in karst areas using the RBM method. Subsequently, the influence of the cavern size and cavern–shaft distance on the stability of the surrounding rock of the shaft was investigated. The following main conclusions can be drawn:

The cavern caused increased radial displacement of the surrounding rock, and the distribution pattern was correlated with the location of the cavern. The influence of the cavern on the radial displacement of the surrounding rock mainly occurs in the range of 20*D*-21*D* above the bottom of the well. The radial stresses in the surrounding rock increase linearly with depth, while the radial stresses in the surrounding rock within 7*D* of the depth of the cavern location are significantly affected by the cavern. On the one hand, the radial displacements of the surrounding rock in different radial orientations have a consistent distribution pattern at the same construction stage and the radial displacements of the surrounding rock increase with the increase in the cavern size. When the cavern size increased from 0 to 2.0*D*, the maximum radial displacement of the surrounding rock in each construction stage increased by 10.7, 16.6, 2.3, and 2.2 times, respectively. On the other hand, the larger the distance between the cavern and the well, the smaller the radial displacement of the surrounding rock at different construction stages. When the distance between the cavern and the well was increased from 0.5*D* to 2.0*D*, the maximum radial displacements of the surrounding rock corresponding to each construction stage were reduced by 51.5%, 61.6%, 40.7%, and 18.4%, respectively. Therefore, the drilling inclination tests should be carried out in real-time during the construction of pilot holes to prevent the drill bit from jamming and deflecting in the karst area. Moreover, real-time monitoring of the stability of the surrounding rock should be carried out during the excavation of deep and large vertical shafts in karst areas using the RBM method.

Author Contributions: Conceptualization, G.W.; methodology, G.W. and F.D.; software, K.R.; validation, G.W.; investigation, Y.F.; data curation, G.W.; writing—original draft preparation, H.X.; writing—review and editing, H.X.; funding acquisition, G.W. All authors have read and agreed to the published version of the manuscript.

Funding: This research was funded by the Department of Transportation Science and Technology of Guizhou Province, grant number No. 2023-122-007.

Data Availability Statement: The original contributions presented in the study are included in the article; further inquiries can be directed to the corresponding author.

Conflicts of Interest: Author Guofeng Wang, Fayi Deng, Kaifu Ren, and Yongqiao Fang were employed by the company Guizhou Road and Bridge Group Co., Ltd. The remaining authors declare that the research was conducted in the absence of any commercial or financial relationships that could be construed as a potential conflict of interest.

References

1. Kaya, A.; Tarakçi, Ü.C. Stability investigation of a deep shaft using different methods. *Int. J. Geomech.* **2021**, *21*, 05020009. [CrossRef]
2. Li, Z.Q.; Lai, J.X.; Ren, Z.D.; Shi, Y.F.; Kong, X.G. Failure mechanical behaviors and prevention methods of shaft lining in China. *Eng. Fail. Anal.* **2023**, *143*, 106904. [CrossRef]
3. Fan, H.B.; Zhou, D.K.; Liu, Y.; Song, Y.X.; Zhu, Z.G.; Zhu, Y.Q.; Gao, X.Q.; Guo, J.Q. Mechanical response characteristics of lining structure of pipeline karst tunnels in water-rich areas. *Rock Soil Mech.* **2022**, *43*, 1884–1898.
4. Cheng, L.; Wang, C.L.; Wang, X.; Chen, K.X. Stability analysis of surrounding rock of large section ultradeep shaft wall. *Adv. Mater. Sci. Eng.* **2021**, *2021*, 4391759.
5. Hou, K.K.; Zhu, M.D.; Hao, Y.J.; Yin, Y.T.; An, L. Stability analysis and evaluation of surrounding rock of ultra-deep shaft under complicated geological conditions. *Front. Earth Sci.* **2023**, *11*, 1216667. [CrossRef]
6. Walton, G.; Kim, E.; Sinha, S.; Sturgis, G.; Berberick, D. Investigation of shaft stability and anisotropic deformation in a deep shaft in Idaho, United States. *Int. J. Rock Mech. Min. Sci.* **2018**, *105*, 160–171. [CrossRef]
7. Tangjarusritaratorn, T.; Miyazaki, Y.; Sawamura, Y.; Kishida, K.; Kimmura, M. Numerical investigation on arching effect surrounding deep cylindrical shaft during excavation process. *Undergr. Space* **2022**, *7*, 944–965. [CrossRef]
8. Wang, Y.S.; Yang, R. Monitoring and analysis of the stress and deformation of shaft lining and the influence of freezing tube fracture in deep topsoil. *Cold Reg. Sci. Technol.* **2022**, *193*, 103420. [CrossRef]
9. Qiao, Y.F.; Xie, F.; Bai, Z.W.; Lu, J.F.; Ding, W.Q. Deformation characteristics of ultra-deep circular shaft in soft soil: A case study. *Undergr. Space* **2024**, *16*, 239–260. [CrossRef]
10. Sun, X.M.; Li, G.; Zhao, C.W.; Liu, Y.Y.; Miao, C.Y. Investigation of deep mine shaft stability in alternating hard and soft rock strata using three-dimensional numerical modeling. *Processes* **2019**, *7*, 2. [CrossRef]
11. Zhang, J.H.; An, L.; Fu, Z.Y.; Li, Y.H. Mechanical response characteristics and stability evaluation of surrounding rock in complex stratum excavation of kilometer deep shaft. *Min. Metall. Explor.* **2024**, *41*, 3241–3256. [CrossRef]
12. Chen, H.; Hou, Y.H.; Wang, W.; Zhang, Y.F. Study on longitudinal deformation profile of shaft under raise-boring method. *J. Shihezi Univ. (Nat. Sci.)* **2021**, *39*, 446–453.
13. Wang, Q.K.; Hu, Z.B.; Guo, Y.J.; Ji, Y.K.; Zhu, B.L.; Ma, J.L. Investigation on uplift behavior of rock-socketed belled piles in horizontal and inclined ground using 1-g model test and 3D numerical method. *Rock Mech. Rock Eng.* **2024**, *57*, 3371–3391. [CrossRef]
14. Vipulanandan, C.; Wong, D.; Ochoa, M.; O'Neill, M.W. Modeling of displacement piles in sand using a pressure chamber. In *Foundation Engineering: Current Principles and Practice*; ASCE: New York, NY, USA, 1989; pp. 526–541.
15. Li, S.C.; Wu, J.; Xu, Z.H.; Zhou, L.; Zhang, B. A possible prediction method to determine the top concealed karst cave based on displacement monitoring during tunnel construction. *Bull. Eng. Geol. Environ.* **2019**, *78*, 341–355. [CrossRef]
16. Lee, J.; You, K.; Jeong, S.; Kim, J. Proposed point bearing load transfer function in jointed rock-socketed drilled shafts. *Soils Found.* **2013**, *53*, 596–606. [CrossRef]
17. Tan, D.M.; Qi, T.Y.; Mo, Y.C. Numerical analysis and research on surrounding rock stability of lateral karst cave tunnel. *Chin. J. Rock Mech. Eng.* **2009**, *28*, 3497–3503.
18. Wu, B.; Sun, W.T.; Cai, G.W.; Meng, G.W. Reliability analysis of shallow-buried tunnel construction adjacent to karst cave. *Comput. Geotech.* **2022**, *145*, 104673. [CrossRef]
19. Huang, F.; Zhao, L.H.; Ling, T.H.; Yang, X.L. Rock mass collapse mechanism of concealed karst cave beneath deep tunnel. *Int. J. Rock Mech. Min. Sci.* **2017**, *91*, 133–138. [CrossRef]
20. Sun, J.L.; Wang, Y.; Wu, X.; Wang, X.L.; Fang, H.; Su, Y. Research on Collapse Risk Assessment of Karst Tunnels Based on BN Self-Learning. *Buildings* **2024**, *14*, 685. [CrossRef]
21. Ma, J.J.; Guan, J.W.; Duan, J.F.; Huang, L.C.; Liang, Y. Stability analysis on tunnels with karst caves using the distinct lattice spring model. *Undergr. Space* **2021**, *6*, 469–481. [CrossRef]

22. Cheng, L.; Yu, L.; Wang, M.N.; Xia, P.X.; Sun, Y. Upper bound analysis of collapse failure of deep tunnel under karst cave considering seismic force. *Soil Dyn. Earthq. Eng.* **2020**, *132*, 106003.
23. Sun, Q.H.; Ma, F.S.; Guo, J.; Li, G.; Feng, X.L. Deformation failure mechanism of deep vertical shaft in Jinchuan mining area. *Sustainability* **2020**, *12*, 2226. [CrossRef]